

# Experimental Investigation of the Thermal Contact Conductance of Electroplated Silver Coatings

M. A. Lambert\* and L. S. Fletcher†  
Texas A&M University, College Station, Texas 77843

Standard electronic modules can be made more reliable by decreasing module temperature. This may be accomplished by increasing the thermal contact conductance of the junction between the frame guide ribs and chassis card rails. Soft metallic coatings for the card rails would deform readily under pressure, thereby increasing the actual contact area and associated conductance. This investigation evaluated the conductance enhancement provided by vapor deposited, electroplated, and flame-sprayed silver coatings. Experimental measurements of thermal contact conductance were performed for anodized aluminum 6101-T6 and electroless nickel-plated copper C11000-H03 frame materials in junction with uncoated and silver-coated A356-T61 card rail material. Baseline conductance data for the anodized aluminum 6101 to uncoated aluminum A356 varied from 25 to 91 W/m<sup>2</sup>K (4.4 to 16 Btu/h ft<sup>2</sup>F), and values for the nickel-plated copper to uncoated aluminum A356 ranged from 600 to 2800 W/m<sup>2</sup>K (106 to 493 Btu/h ft<sup>2</sup>F) for contact pressures of 172–862 Kpa (25 to 125 psi) and mean junction temperatures of 20–100°C (68–212°F). Experimental conductance data for vapor-deposited, electroplated, and flame-sprayed silver-coated aluminum A356 demonstrated thermal enhancement factors of 1.44–2.14, 1.78–15.2, and 1.00–2.30, respectively, for junctions with anodized aluminum 6101, and 0.76–2.19, 1.06–2.83, and 0.45–0.75, respectively, for junctions with nickel-plated copper. The vapor deposited and thinner flame-sprayed coatings were susceptible to galvanic corrosion. All electroplated and the thicker flame-sprayed coatings exhibited excellent corrosion resistance.

## Nomenclature

$F$  = flatness  
 $H$  = Vicker's microhardness  
 $h$  = thermal contact conductance  
 $k$  = thermal conductivity  
 $R$  = roughness  
 $S$  = asperity slope  
 $t$  = coating thickness  
 $W$  = waviness

## Subscripts

$a$  = average  
 $c$  = coated, coating  
 $q$  = rms  
 $s$  = substrate  
 $u$  = uncoated

## 1. Introduction

THE performance of electronics is often diminished by excessive operating temperatures, as evidenced by increased switching times and rates of failure.<sup>1</sup> The thermal contact resistance between the frame guide ribs and chassis card rails of standard electronic module (SEM) systems, shown in Fig. 1, which are utilized extensively in electronic systems, present a significant barrier to heat rejection. Heat transfer across pressed junctions (e.g., the guide rib/card rail junction) is restricted because the true contact area is only a small fraction of the apparent contact area, due to irregularities in surface profile, which limit contact to a relatively few small

spots.<sup>2</sup> As a result, heat is constrained to pass primarily through narrow constrictions or bridges of contact between the two surfaces. This restriction is manifested by a large change in temperature across the gap between two contacting surfaces.

The thermal contact resistance at a junction between two materials may be reduced by a number of methods. These include, increasing the apparent contact area, using smoother, flatter surfaces, increasing the contact pressure, and inserting or applying certain foils or coatings between the surfaces. Augmenting the apparent contact area may require extensive system redesign, finer surface finishes, and closer tolerances that may not be economically or technologically feasible, and excessive contact pressure that may damage or distort components. Thus, conductance enhancing interstitial materials comprise an attractive alternative. Soft, conductive foils and coatings may enhance the contact conductance by deforming readily under load, thereby conforming to the surfaces and increasing the contact area. Fletcher<sup>3</sup> performed an extensive

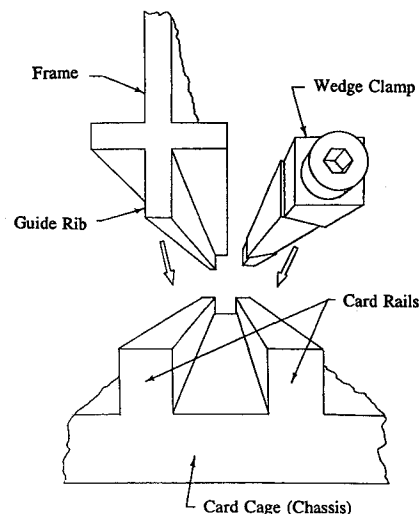


Fig. 1 Exploded view of SEM junction.

Presented as Paper 93-0846 at the AIAA 31st Aerospace Sciences Meeting and Exhibit, Reno, NV, Jan. 11–14, 1993; received June 4, 1993; revision received June 1, 1994; accepted for publication June 6, 1994. Copyright © 1994 by the American Institute of Aeronautics and Astronautics, Inc. All rights reserved.

\*Graduate Research Assistant, Conduction Heat Transfer Laboratory, Department of Mechanical Engineering. Student Member AIAA.

†Thomas A. Dietz Professor, Conduction Heat Transfer Laboratory, Department of Mechanical Engineering. Fellow AIAA.

review of investigations dealing with thermal enhancement techniques for electronic components, and concluded that soft metallic interstitial materials provided the greatest thermal enhancement. He also surmised that metallic coatings are superior to metallic foils and inserts because coatings are typically more durable and not subject to wrinkling, the occurrence of which may actually increase contact resistance.

The purpose of the present investigation is that of enhancing the contact conductance of the junction between the frame guide rib and chassis card rail of SEM systems, more specifically, identifying and characterizing the most suitable metallic coating for the chassis card rails. A more detailed account of this investigation has been reported by Lambert and Fletcher.<sup>4</sup> The electronic modules may be subjected to harsh environmental conditions, such as sliding contact during insertion and removal of frames, periodic contact due to thermal cycling, severe vibrational and accelerative loading (in avionics), and corrosive (marine) atmospheres. Therefore, any potential metallic coating material for aluminum card rails must be not only corrosion-resistant, when used singly, but must be also galvanically compatible with metallic frame materials with which it is in contact.

There have been a number of experimental investigations dealing with the thermal contact conductance of metals with metallic coatings.<sup>5-17</sup> All but one of these investigations involved the use of vapor-deposited or ion-deposited metallic or metal/carbon coatings. Mal'kov and Dobashin<sup>7</sup> performed the only contact conductance experiments with electrochemically plated surfaces (i.e., silver, nickel, and copper platings on stainless steel). Chung et al.<sup>14</sup> and Sheffield et al.<sup>15</sup> studied the conductance of transitional buffering interface (TBI) coatings. These coatings are composed of phase mixtures of vapor-deposited carbon and metals (e.g., copper/carbon and silver/carbon). Some of these investigations contain theoretical correlations for predicting the thermal contact conductance of metallic-coated metals. However, as previously described,<sup>18</sup> these correlations are not generally applicable to the majority of published data.

Lambert and Fletcher<sup>18</sup> reviewed the properties of all metallic elements with the purpose of identifying those most suitable for SEM card rails. They concluded that all but silver and gold should be excluded from consideration for reasons of high hardness, poor wear resistance, low conductivity, galvanic incompatibility with the electroless nickel-plated frame, or poor corrosion resistance. Gold, as a coating for the card rails, would be prohibitively expensive, because of the quantities of the metal required, leaving silver as the best overall choice.

The hardness and surface finish of metallic coatings, which have a significant effect on their contact conductance, are greatly dependent upon the method of application. Vapor-deposited metallic or TBI coatings are typically quite soft. Vibrational loading and repeated contact during thermal cycling or assembly and disassembly may wear away such coatings. Lambert and Fletcher<sup>15</sup> demonstrated the susceptibility of vapor-deposited silver and gold coatings on aluminum substrates to galvanic corrosion, probably due to the presence of pinholes in the thin metallic coatings. Another possible drawback to the use of vapor-deposited metallic or TBI coatings for large or intricate components is the fact that these coatings must be applied in vacuo, and the path between the vapor source and the surface to be coated must be largely unobstructed. Consequently, vapor-deposited metallic or TBI coatings may not be viable conductance-enhancing coatings for SEM card rails.

The conductance enhancing capability of electroplated metallic coatings has been largely unexplored. Electroplated metallic coatings often exhibit excellent adhesion to the substrate and good corrosion and wear resistance, depending on the nature and thickness of the plating. Pinhole-free platings of sufficient thickness completely mask the substrate, thereby preventing galvanic corrosion between the plating and sub-

strate. The method of plating lends itself to use with large, intricate components and high-volume production.

Plasma (or flame) spraying is another coating method that may produce durable, adherent coatings. Plasma spraying involves injecting metal powders (or feeding metal wire in the case of flame spraying) into a high velocity stream of combustion gases that melt the metal and propel it onto the surface to be coated.

This investigation was directed toward experimental measurement of the thermal contact conductance for anodized aluminum 6101-T6 and electroless nickel-plated copper C11000-H03 frame materials in contact with bare aluminum A356-T61 card rail material, then experimental determination of the conductance when the aluminum A356 was coated with vapor-deposited, electroplated, and flame-sprayed silver.

## II. Experimental Program

An experimental investigation of the thermal contact conductance of silver coatings for SEM card rails has been conducted. The experimental facility, materials, samples, coating techniques, corrosion-resistance testing, thermophysical property measurements, test procedure, and data and uncertainty analyses are described below.

### A. Experimental Facility

The experimental apparatus consists of a frame that supports the contact conductance test specimens (hereafter called heat flux meters) in a vertical column, as shown in Fig. 2. It contains a pneumatic pressure bellows for applying the desired contact load and a load cell for measuring this load. The upper and lower fixtures (source-sink-holder assemblies) are each equipped with electrical heaters and a coolant jacket through which refrigerated ethylene glycol from a constant temperature bath may be circulated. The upper heat flux meter is inserted into the upper fixture, the lower heat flux meter is inserted into the lower fixture, and the middle heat flux meter is placed between the upper and lower heat flux meters.

Load is transferred from the lower movable plate and the base plate to the specimen column through a pair of stainless steel ball bearings, one atop the upper fixture and the other beneath the lower fixture. The ball bearings serve to maintain uniform axial loading across the test surfaces by eliminating bending moments. Flexible hoses supplying the coolant jackets nearly eliminate lateral forces and their associated bending moments.

A heat flux may be established in either the upward or downward direction by providing power to the heaters in one fixture and supplying refrigerant to the other fixture. The

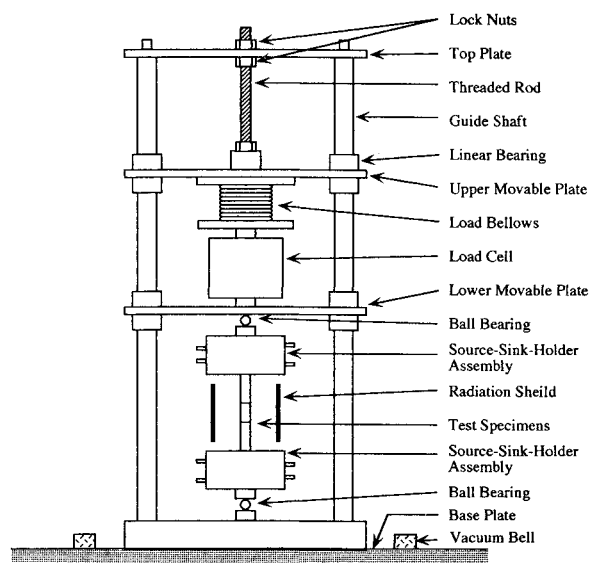


Fig. 2 Experimental apparatus.

**Table 1 Thermal conductivity, Vicker's microhardness, and surface metrological data for test specimens**

Base material-sample-surface <sup>a</sup>	Coating material	$ks/kc$ , <sup>b</sup> W/mK	$H_u/H_c$ , <sup>c</sup> kg/mm <sup>2</sup>	$t$ , $\mu$ m	$Ra$ , $\mu$ m	$Rq$ , $\mu$ m	$Wa$ , $\mu$ m	$Wq$ , $\mu$ m	$F$ , $\mu$ m	$t$ , $\mu$ in.	$Ra$ , $\mu$ in.	$Rq$ , $\mu$ in.	$Wa$ , $\mu$ in.	$Wq$ , $\mu$ in.	$F$ , $\mu$ in.
6101-F2	Anodized hard coat	208.4/0.0292	85/280	85.1	2.09	2.70	1.44	1.88	26.95	3350	82.3	106.3	56.7	74.0	1061
					1.98	2.61	1.25	1.58	26.30		78.0	102.8	49.2	62.2	1035
C110-F2	Electroless nickel plating	405.7/5.02	101/600	44.3	0.12	0.16	0.77	0.86	4.45	1744	4.7	6.3	30.3	33.9	175
					0.14	0.19	1.17	1.31	5.75		5.5	7.5	46.1	51.6	226
A356-S3-AA	Bare	152.1/None	128/None	0	1.04	1.20	0.55	0.67	9.10	0	40.9	47.2	21.7	26.4	358
A356-S3-NC				0	0.30	0.41	0.21	0.26	5.75	0	11.8	16.1	8.3	10.2	226
A356-S5-AA	Vapor-deposited silver	152.1/427	128/116	1.00	0.69	0.81	0.40	0.49	7.30	39.4	27.2	31.9	15.7	19.3	287
A356-S5-NC				1.00	0.25	0.34	0.24	0.32	4.55	39.4	9.8	13.4	9.4	12.6	179
A356-S4-AA			128/108	2.00	0.15	0.22	0.58	0.70	5.10	78.6	5.9	8.7	22.8	27.6	201
A356-S4-NC				2.00	0.23	0.31	0.30	0.38	4.30	78.7	9.1	12.2	11.8	15.0	169
A356-S6-AA			128/101	3.00	0.35	0.44	0.39	0.52	4.55	118.0	13.8	17.3	15.4	20.5	179
A356-S6-NC				3.00	0.52	0.63	0.34	0.42	6.00	117.9	20.5	24.8	13.4	16.5	236
A356-S14-AA	Electroplated-silver	152.1/427	128/83	12.7	1.40	1.80	0.71	0.88	19.05	500	55.1	70.9	28.0	34.6	750
A356-S14-NC				12.7	1.52	1.90	1.69	2.38	23.95	500	59.8	74.8	66.5	93.7	943
A356-S19-AA			128/95	25.4	1.97	2.66	0.97	1.21	30.45	1000	77.6	104.7	38.2	47.6	1199
A356-S19-NC				25.4	2.18	2.83	0.61	0.74	32.40	1000	85.8	111.4	24.0	29.1	1276
A356-S18-AA			128/93	50.8	1.38	1.80	0.99	1.28	19.80	2000	54.3	70.9	39.0	50.4	780
A356-S18-NC				50.8	1.37	1.76	0.87	1.05	27.35	2000	53.9	69.3	34.3	41.3	1077
A356-S17-AA			128/93	76.2	1.48	1.88	1.69	2.35	24.10	3000	58.3	74.0	66.5	92.5	949
A356-S17-NC				76.2	1.17	1.50	1.22	1.66	20.50	3000	46.1	59.1	48.0	65.4	807
A356-S8-AA	Flame-sprayed silver	152.1/427	128/115	12.7	7.65	9.46	2.80	3.58	65.15	500	301.2	372.4	110.2	140.9	2565
A356-S8-NC				12.7	6.13	7.59	2.61	3.26	56.00	500	241.3	298.8	102.8	128.3	2205
A356-S7-AA			128/117	25.4	6.90	8.55	3.89	5.08	72.80	1000	271.7	336.6	153.1	200.0	2866
A356-S7-NC				25.4	6.21	7.74	3.55	4.68	90.10	1000	244.5	304.7	139.8	184.3	3547
A356-S21-AA			128/112	50.8	5.96	7.39	3.50	4.37	71.40	2000	234.6	290.9	137.8	172.0	2811
A356-S21-NC				50.8	5.19	6.37	4.22	5.65	61.55	2000	204.3	250.8	166.1	222.4	2423
A356-S20-AA			128/113	76.2	6.74	8.28	4.51	5.52	86.85	3000	265.4	326.0	177.6	217.3	3419
A356-S20-NC				76.2	5.00	6.16	6.78	8.06	68.35	3000	196.9	242.5	266.9	317.3	2691

<sup>a</sup>AA and NC denote surfaces in contact with anodized aluminum 6101 and nickel-plated copper, respectively. The two rows of data for the anodized aluminum 6101 and copper specimens are for mutually perpendicular measurements across each of their surfaces.

<sup>b</sup> $k$  for anodic coating from Peterson and Fletcher,<sup>21</sup>  $k$  for nickel plating from Gawrilov,<sup>22</sup> and  $k$  for silver from Touloukian and Ho.<sup>20</sup>

<sup>c</sup> $H_u$  is VHN of uncoated substrate material, and  $H_c$  is VHN of coating/substrate combination. As a point of reference, Tabor<sup>23</sup> lists the hardness of annealed silver as 25 kg/mm<sup>2</sup>.

apparatus is housed in a vacuum chamber, which is maintained at  $10^{-5}$  Torr by a Varian VHS-6 oil diffusion pump in series with an Alcatel 2300 rotary pump, to reduce convective heat loss to a negligible level. A passive radiation shield made from reflective aluminum foil is installed around the specimens to further reduce heat losses.

#### B. Specimens (Heat Flux Meters)

All heat flux meters are cylindrical with a diameter of 2.54 cm (1.0 in.). The upper and lower heat flux meters are 10.16 cm (4.0 in.) long and are fabricated from anodized aluminum 6101-T6 and electroless nickel-plated copper C11000-H03, respectively. The anodized coating is estimated to be 85.1  $\mu$ m (0.00335 in.) thick and the electroless nickel plating is 44.29  $\mu$ m (0.001744 in.) thick. The middle heat flux meter is 3.81 cm (1.5 in.) long and is made of aluminum A356 that is either bare on both ends or coated on both ends with silver in selected thicknesses. Each heat flux meter has five 0.118-cm- (0.0465-in.-) diam holes drilled along radii to its centerline at intervals of 0.635 cm (0.25 in.). Into each hole is inserted a 30-gauge Teflon<sup>®</sup>-insulated chromel-alumel (type K) thermocouple. The thermocouples are special limit-of-error grade [ $\pm 1.1^\circ\text{C}$  ( $2^\circ\text{F}$ ), one-half of normal], although the variation between thermocouples fabricated from a single spool of wire is typically on the order of  $0.05^\circ\text{C}$  ( $0.09^\circ\text{F}$ ) or less. Each thermocouple is secured in place with metal powder to match the specimen material. The metal powder provides good thermal contact between the thermocouple bead and the entire periphery of the hole.

#### C. Thermal Conductivity Calibration

The thermal conductivity of a sample of each of the three base materials (aluminum alloys A356-T61 and 6101-T6, and copper C11000-H03) was determined using the contact conductance apparatus because accurate values of conductivity are needed to calculate the heat flux across the test junctions.

For the purpose of measuring thermal conductivity, a heat flux meter fabricated from each of the three base materials was used alternately as the middle heat flux meter in the test column. The upper and lower heat flux meters (aluminum 6101 and copper, respectively) were replaced by a pair of electrolytic iron heat flux meters machined to the previously described configuration. The thermal conductivity of the electrolytic iron over a wide range of temperature was measured by the National Bureau of Standards/National Institute of Standards and Technology (NBS/NIST).<sup>19</sup> Thus, the conductivity of the base materials is traceable to a universally accepted standard. The experimentally determined values of thermal conductivity and Vickers microhardness (VHN) for the three base materials approximate published values for similar alloys<sup>20-23</sup> and are listed in Table 1.

#### D. Coating Techniques

The aluminum 6101 heat flux meter, as well as coating thickness and hardness test coupons, were given a black anodic coating using a chilled sulfuric acid process described by Darrow.<sup>24</sup> "Hard coat" is the term commonly used in industry (Type III in U.S. military specifications) to describe anodic coatings synthesized by this technique. The electroless (i.e., no electrical current applied) nickel plating for the copper C11000-H03 heat flux meter and test coupons was deposited using methods described by Krieg<sup>25</sup> and a plating solution developed by Maclean and Karten.<sup>26</sup>

The vapor-deposited silver coatings for the aluminum A356 were applied by placing the heat flux meters and hardness coupons to be coated in a vacuum chamber near an evaporation source containing silver. The evaporated metal coats the flux meter or coupon (and all other surfaces in the vacuum chamber) by condensing on the sample.

The method of electroplating the silver onto the A356 aluminum involves two steps, a preliminary, thin, silver "strike" coating, and a subsequent thicker main plating. The strike coating is essential for good adhesion of the main plating.

The main plating electrolyte is that described by Sora and Bollhalder,<sup>27</sup> and the strike formula is that given by Blair.<sup>28</sup>

The flame-sprayed silver coatings were applied by the high-velocity oxygen fuel (HVOF) method. This involves igniting a high-pressure fuel ( $H_2$ ) and oxygen mixture in a combustion chamber and directing the hot gas through a channeling nozzle. Silver wire is fed into the hot gas stream near the tip of the nozzle where it is melted and propelled by the gas jet onto the surface to be coated.

#### E. Microhardness Measurements

The VHN of the three base materials and all coating/base material combinations used in this investigation was measured using a Buehler microhardness tester with indenter loads ranging from 10- to 500-g force. The microhardness values for a load of 500-g force are listed in Table 1.

The VHN of the electroless nickel-plated copper C11000-H03 for platings thicker than  $34\text{ }\mu\text{m}$  (0.0014 in.) was determined to range from 530 to 640  $\text{kg/mm}^2$ , which is within the published range expected for such coatings (500–700  $\text{kg/mm}^2$ ).<sup>22</sup> The microhardness of platings thinner than  $34\text{ }\mu\text{m}$  (0.0014 in.) decreases with increasing indenter load because the indenter penetrates the plating deeply enough for the soft copper substrate to influence the indicated hardness. Since the electroless nickel plating applied to the copper specimen is  $44.3\text{ }\mu\text{m}$  (0.00174 in.) thick, its VHN is estimated to be approximately 600  $\text{kg/mm}^2$ .

The VHN of the anodized coating is generally independent of indenter load and increases slightly with coating thickness. The value of 280  $\text{kg/mm}^2$  listed in Table 1 is the average determined for a hard coat sample approximately  $85\text{ }\mu\text{m}$  (0.00335 in.) thick.

All three types of silver coating/aluminum A356 combinations yielded lower VHN values than the VHN of bare aluminum A356. The electroplated silver-coated aluminum A356 was the softest of the three combinations, and the microhardness varied little with coating thickness. The microhardness of vapor-deposited silver-coated aluminum A356 decreased slightly with increasing coating thickness. The VHN of the flame-sprayed silver-coated aluminum A356 was essentially independent of coating thickness and the greatest of the three types of silver coating/aluminum combinations.

#### F. Surface Measurements

The topography of contacting surfaces has a profound effect on the thermal contact conductance of the junction. Consequently, the specimen's surfaces were characterized using a Surfanalyzer 5000/400 manufactured by Federal Products Corporation. Salient surface measurements are provided in Table 1.

#### G. Environmental Testing

Samples of all coating/substrate combinations used in this investigation were subjected to the standard salt spray test as per ASTM Standard B117.<sup>29</sup> The salt spray test provides an accelerated (48-h) trial of component performance in a marine environment.

After exposure, no evidence of corrosion was found on the anodized aluminum 6101 and electroless nickel-plated copper coupons. However, the vapor-deposited silver-coated A356 coupons exhibited extensive flaking of the coating and oxidation of the substrate, indicative of poor adhesion and galvanic corrosion. Coupons with thin flame-sprayed silver coatings also corroded, probably because the thin flame-sprayed coatings, which are highly porous, did not completely cover the aluminum substrate. The electroplated silver-coated coupons displayed no indications of corrosion.

#### H. Experimental Procedure

Each separate test began with insertion of the bare or coated aluminum A356 middle heat flux meter between the anodized aluminum 6101 upper heat flux meter and the electroless nickel-

plated copper lower heat flux meter. Exact alignment of the specimens was ensured by use of a specially designed alignment tool. A preload pressure of 862 kPa (125 psi), equal to the maximum-test pressure, was applied to simulate the standard practice of applying maximum-rated torque to wedge clamps, then pressure was reduced to the minimum test pressure of 172 kPa (25 psi).

All thermocouples were connected to a Hewlett Packard 3497A data acquisition system, the radiation shield was placed around the test column, and the vacuum jar was then sealed over the apparatus and evacuated. After outgassing, the appropriate coolant valve was opened, bellows pressure adjusted, and heater power selected. Contact pressure was increased from 172 to 862 kPa (25 to 125 psi) while maintaining each desired mean interface temperature, which was in turn raised from 20 to 100°C (68 to 212°F). Thus, counting the preloading as the first cycle, the 20°C test was the second cycle, the 40°C test was the third cycle, etc. Steady-state was assumed to have been obtained when none of the temperature readings of the 15 thermocouples changed by more than 0.3°C within an hour. The data acquisition system was used to collect temperature data, which was transmitted to an HP-87 computer that calculated the thermal contact conductance values.

#### I. Data Analysis

The conductance evaluation program utilized temperature and load measurements, and heat flux meter configurations and conductivities. The program calculated the heat flux through each of the three heat flux meters from Fourier's Law, using its temperature gradient, obtained from a linear regression of its five thermocouple temperature readings, and its previously calibrated temperature-dependent conductivity. The temperature discontinuities across the junctions were obtained by extrapolating the temperature profiles within the heat flux meters to the interfaces. The contact conductance of the appropriate junction, for which heat passed from either the anodized aluminum 6101 upper heat flux meter or the electroless nickel-plated copper lower heat flux meter (frame material) to the aluminum A356 middle heat flux meter (card rail material), was computed as the average heat flux of the specimens on either side of the junction divided by the temperature discontinuity across the junction.

#### J. Uncertainty Analysis

Uncertainty in the experimentally determined thermal contact conductance data arises from a number of causes, the major contributors being uncertainties in the thermal conductivity of the specimens and errors in the indicated thermocouple temperatures due to their limit of accuracy and electrical signal noise in the instrumentation. Since the level of uncertainty must be considered when evaluating the experimental results, the method of Kline and McClintock<sup>30</sup> is used to estimate the uncertainty in the conductance data.

The uncertainties in the thermal conductivities of the three base materials were calculated to be 2.38, 3.14, and 5.30% for the aluminum A356-T61, aluminum 6101-T6, and copper C11000-H03, respectively. The uncertainty in the contact conductance is estimated to be 6.07% for the anodized aluminum 6101 to bare aluminum A356, and 9.28% for the electroless nickel-plated copper to bare aluminum A356. The uncertainty in the contact conductance for junctions involving silver-coated aluminum A356 is 6.44%.

### III. Results and Discussion

In order to assess the potential enhancement of thermal contact conductance afforded by silver coatings for the card rails, baseline data for junctions with uncoated card rail material were needed for comparison with results for junctions with silver-coated card rail material. This investigation entailed the experimental determination of the thermal contact conductance for anodized aluminum 6101-T6 and electroless nickel-plated copper C11000-H03 frame materials in contact

with bare aluminum A356-T61 card rail material, as well as experimental measurement of the conductance for vapor-deposited, electroplated, and flame-sprayed silver-coated aluminum A356-T61. The contact conductance data for junctions involving bare and vapor-deposited silver-coated aluminum A356 were determined previously.<sup>16</sup> These results are discussed here for the purpose of comparing them to the conductance data for electroplated and flame-sprayed silver coatings and to an existing predictive theory.<sup>10</sup>

#### A. Baseline Contact Conductance Results

The thermal contact conductance data for the anodized aluminum 6101-T6 and electroless nickel-plated copper C11000-H03 in junction with bare aluminum A356 are presented in Fig. 3 as a function of apparent contact pressure and mean interface temperature. The thermal contact conductance for the anodized aluminum 6101 to bare aluminum A356 ranges from 25 to 92 W/m<sup>2</sup>K (4.4 to 16 Btu/h-ft<sup>2</sup>°F) over the given ranges of temperature and pressure. The relatively low magnitude of the conductance is reasonable, since the anodic coating is a very poor conductor and so acts as an insulator, and its relatively high hardness and large roughness (see Table 1) result in a very small true contact area.

Peterson and Fletcher<sup>21</sup> performed one of the few other experimental investigations of the thermal conductivity and thermal contact conductance of anodized aluminum. They tested aluminum 6061-T6 with anodic coatings of several different thicknesses in contact with bare aluminum. Some of the anodic coatings they studied were comparable in thickness to the anodic coating used in the present investigation, i.e., 84.3  $\mu\text{m}$  (0.00332 in.), and the conductance data for these coatings are included in Fig. 3. The magnitude and trends of the data are similar. Peterson and Fletcher<sup>21</sup> performed all tests at a mean interface temperature of 25°C (77°F). They did not describe the particular anodization process for their specimens.

The thermal contact conductance of the nickel-plated copper C11000-H03 to aluminum A356 varies from 600 to 2800 W/m<sup>2</sup>K (106 to 493 Btu/h-ft<sup>2</sup>°F), which is substantially (25 to

30 times) greater than the conductance of the anodized aluminum 6101 to bare aluminum A356. Although the electroless nickel-plated copper is approximately twice as hard as the anodized aluminum 6101, it is the hardness of the softer material (bare aluminum A356 in both cases) that has a greater effect on contact conductance, as it is the first to undergo plastic flow. The conductance of the nickel-plated copper to bare aluminum A356 is much greater than the conductance of the anodized aluminum 6101 to bare aluminum A356, because the nickel plating is many times more conductive and much smoother than the anodic coating.

For both junctions, the contact conductance increases significantly with increasing temperature. This may be due in part to increased conductivity of the materials and softening of the aluminum A356 (the nickel plating and anodic coating do not soften from 20 to 100°C), although the moderate changes in these properties can account for only a small portion of the substantial increase in conductance with temperature. Thermally induced distortions of the nonconforming surfaces may contribute to the increase, although over the moderate temperature range employed, this effect is not expected to be very large. The major contributor to this phenomenon is very likely repeated loading. Although a preload equal to the maximum test load was employed after insertion of each aluminum A356 middle heat flux meter, plastic deformation and, hence, true contact area, may have been increased with each successive pressure excursion. Recall that testing began with increasing pressure while maintaining 20°C, followed by reducing pressure to the minimum value, raising temperature 40°C, then again increasing pressure, etc.

#### B. Contact Conductance for Vapor-Deposited Silver Coatings

The thermal contact conductance data for anodized aluminum 6101 and electroless nickel plated copper in contact with vapor-deposited silver-coated aluminum A356 are illustrated in Fig. 4 as a function of coating thickness, contact pressure, and mean interface temperature. Vapor-deposited

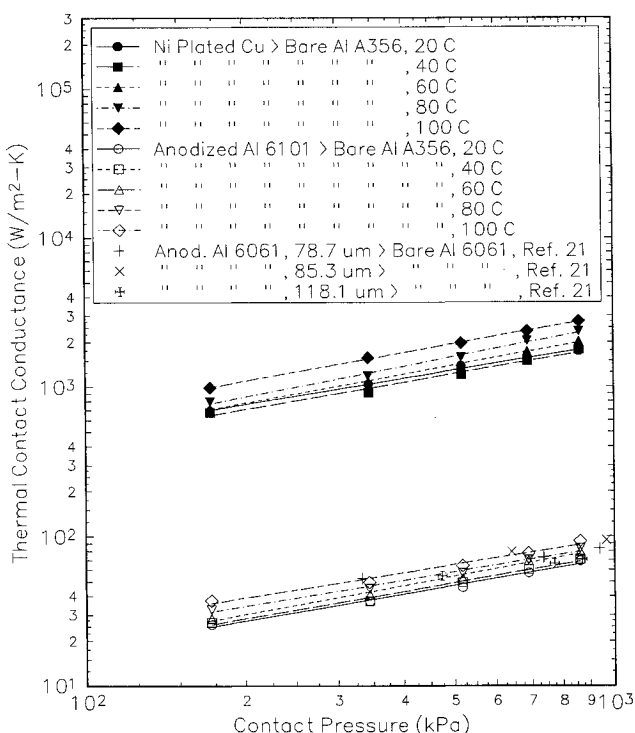


Fig. 3 Thermal contact conductance of anodized aluminum 6101-T6 to uncoated aluminum A356-T61 and electroless nickel-plated copper C11000-H03 to uncoated aluminum A356-T61 with a comparison to published data.

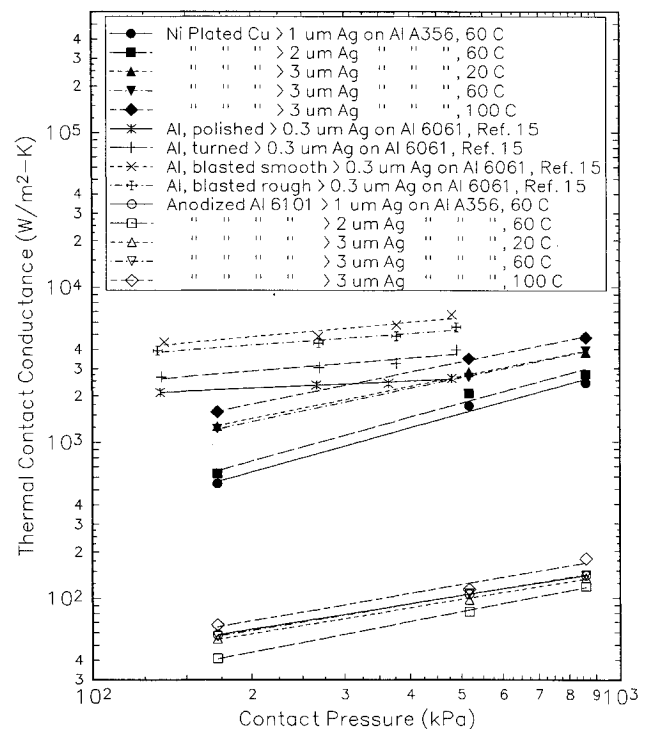


Fig. 4 Thermal contact conductance of anodized aluminum 6101-T6 to vapor-deposited silver-coated aluminum A356-T61 and electroless nickel-plated copper C11000-H03 to vapor-deposited silver-coated aluminum A356-T61 for selected coating thicknesses with a comparison to published data.

silver was applied to the aluminum A356 in thicknesses of 1, 2, and 3  $\mu\text{m}$  (39, 79, and 118  $\mu\text{in.}$ , respectively).

Thermal contact conductance is expected to increase with increasing coating thickness (for coatings softer than the substrate) until the coating is sufficiently thick that its bulk resistance becomes significant, as stated by Kang et al.<sup>12</sup> They noted that the optimum thickness of indium, lead, and tin coatings ranged from 0.5 to 2  $\mu\text{m}$ . Silver is the most highly conductive metal and would have to be applied in much greater thicknesses than used in this investigation for its bulk resistance to have a measurable effect on conductance.

However, for the junction of anodized aluminum 6101 to vapor-deposited silver-coated aluminum A356, the conductance of the 2- $\mu\text{m}$  vapor deposited silver coating is less than the conductance of the 1- $\mu\text{m}$  coating. This is because the 2- $\mu\text{m}$  silver-coated surface exhibited significant crowning or rounding, thereby reducing the size of the macroscopic contact region, whereas the 1- $\mu\text{m}$ -coated heat flux meter was quite flat, allowing contact over nearly its entire surface. The 3- $\mu\text{m}$ -coated surface was also rounded, though less so than the 2- $\mu\text{m}$ -coated surface, which may account for the fact that the conductance of the 3- $\mu\text{m}$ -coated surface was only slightly greater than that of the 1- $\mu\text{m}$  coating. The 3- $\mu\text{m}$  coating was selected for further testing at 20 and 100°C. Note from Fig. 4 that the conductance of the anodized aluminum 6101 to 3- $\mu\text{m}$  silver-coated aluminum A356 increases considerably with increasing temperature.

As shown in Fig. 4, the conductance of the nickel-plated copper to vapor-deposited silver-coated aluminum A356 junction increases monotonically with silver-coating thickness. The 1- $\mu\text{m}$ -coated surface was very flat, while the 2- and 3- $\mu\text{m}$ -coated surfaces showed slight rounding. The 3- $\mu\text{m}$  coating was also tested at 20 and 100°C, and, again, the conductance increased significantly with increasing temperature.

Also shown in Fig. 4 are contact conductance data for vapor-deposited silver-coated aluminum 6061-T651 in contact with bare aluminum 6061-T651 from Sheffield et al.<sup>15</sup> These data were obtained at a mean interface temperature of 60°C for silver coatings of 0.3  $\mu\text{m}$  (12  $\mu\text{in.}$ ) average thickness on specimens of widely varying roughness, 0.25–4.4  $\mu\text{m}$  (10–176  $\mu\text{in.}$ ), as indicated by their surface descriptions in Fig. 6. The data reported by Sheffield et al.<sup>15</sup> are considerably greater in magnitude than the results of the present investigation. This may be because the aluminum 6061-T651 specimens they tested were probably of lower hardness than the aluminum A356 employed in this investigation, as evidenced by their bare junction results (not shown), which are considerably greater than the bare junction results for the present investigation. Their specimens also may have been flatter, resulting in larger macroscopic contact regions. The results of Sheffield et al.<sup>15</sup> show an increase in conductance with increasing roughness.

### C. Contact Conductance for Electroplated Silver Coatings

The thermal contact conductance data for anodized aluminum 6101 and electroless nickel-plated copper to electroplated silver-coated aluminum A356 are plotted in Fig. 5. Four thicknesses of electroplated silver were tested, 12.7, 25.4, 50.8, and 76.2  $\mu\text{m}$  (0.0005, 0.001, 0.002, and 0.003 in., respectively).

Figure 5 shows that the conductance of the thinnest electroplated coating (12.7  $\mu\text{m}$ ) in contact with the anodized aluminum 6101 is several times greater than the conductance of the thicker electroplatings, and that conductance generally decreases with increasing plating thickness. This may be due to the fact that the plating process generated localized spots with a significantly greater plating thickness than the rest of the surface. These raised spots or bumps, which were essentially absent from the 12.7- $\mu\text{m}$  plating, increased in size with increased plating thickness. Contact was mostly limited to the tops of these raised spots, which caused the conductance of the three thicker platings to be much lower than the conductance of the 12.7- $\mu\text{m}$  plating. The 12.7- $\mu\text{m}$  silver-plated

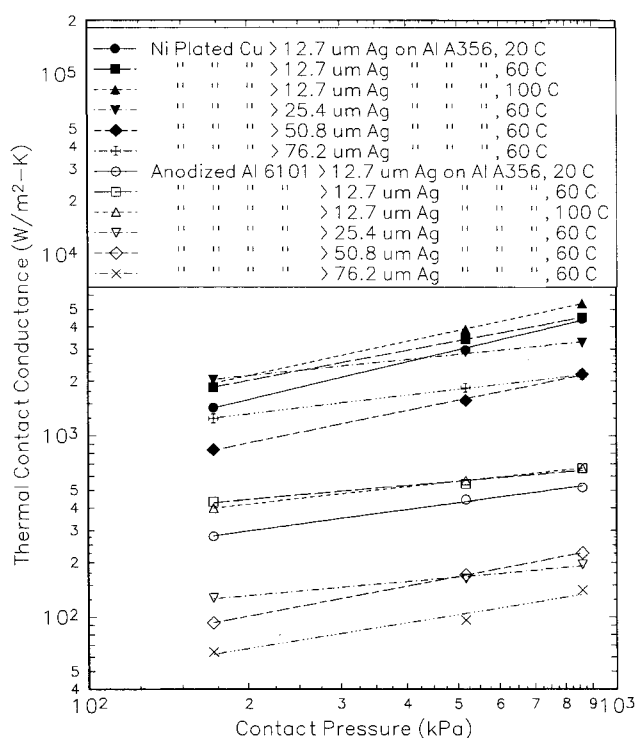


Fig. 5 Thermal contact conductance of anodized aluminum 6101-T6 to electroplated silver-coated aluminum A356-T61 and electroless nickel-plated copper C11000-H03 to electroplated silver-coated aluminum A356-T61 for selected coating thicknesses.

surface was also tested at 20 and 100°C. Note that the conductance of the 12.7- $\mu\text{m}$  plating in contact with the anodized aluminum 6101 increases markedly from 20 to 100°C.

The thinnest electroplated silver coating (12.7  $\mu\text{m}$ ) for the aluminum A356 also yielded the greatest conductance in contact with the nickel-plated copper, as seen in Fig. 5. Again, this was due to the presence of bumps on the thicker silver platings, which impeded heat flow across the junction. The conductance generally decreased with increasing coating thickness. Again, the 12.7- $\mu\text{m}$  electroplated silver coating was tested at 20 and 100°C, and the conductance was found to increase considerably with increasing temperature.

### D. Contact Conductance for Flame-Sprayed Silver Coatings

Thermal contact conductance data for the anodized aluminum 6101 and electroless nickel-plated copper in contact with flame-sprayed silver-coated aluminum A356 are shown in Fig. 6. Four thicknesses of flame-sprayed silver were evaluated, 12.7, 25.4, 50.8, and 76.2  $\mu\text{m}$  (0.0005, 0.001, 0.002, and 0.003 in., respectively).

As illustrated in Fig. 6, the thinnest flame-sprayed silver coating (12.7  $\mu\text{m}$ ) for the aluminum A356 provided the greatest thermal contact conductance in junction with the anodized aluminum 6101. Hence, this coating thickness was also tested at 20 and 100°C. The conductance increases considerably with increasing temperature.

The 12.7- and 50.8- $\mu\text{m}$ -thick flame-sprayed coatings for the aluminum A356 in junction with the nickel-plated copper (Fig. 6) displayed the greatest conductance values over the range of pressures tested. The 12.7- $\mu\text{m}$  coating was chosen for further testing at 20 and 100°C. Again, the conductance is observed to increase markedly with increasing temperature.

### E. Thermal Enhancement Provided by Silver Coatings

The contact conductance for anodized aluminum 6101 to vapor-deposited, electroplated, and flame-sprayed silver-coated aluminum A356 with respect to the conductance for anodized aluminum 6101 to uncoated aluminum A356 (i.e., ratio of coated to uncoated conductance) is plotted in Fig. 7. The

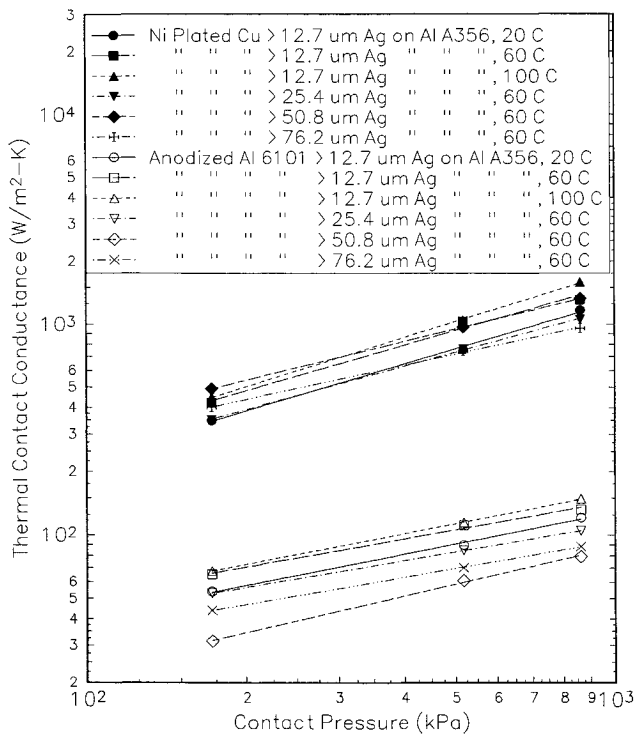


Fig. 6 Thermal contact conductance of anodized aluminum 6101-T6 to flame-sprayed silver-coated aluminum A356-T61 and electroless nickel-plated copper C11000-H03 to flame-sprayed silver-coated aluminum A356-T61 for selected coating thicknesses.

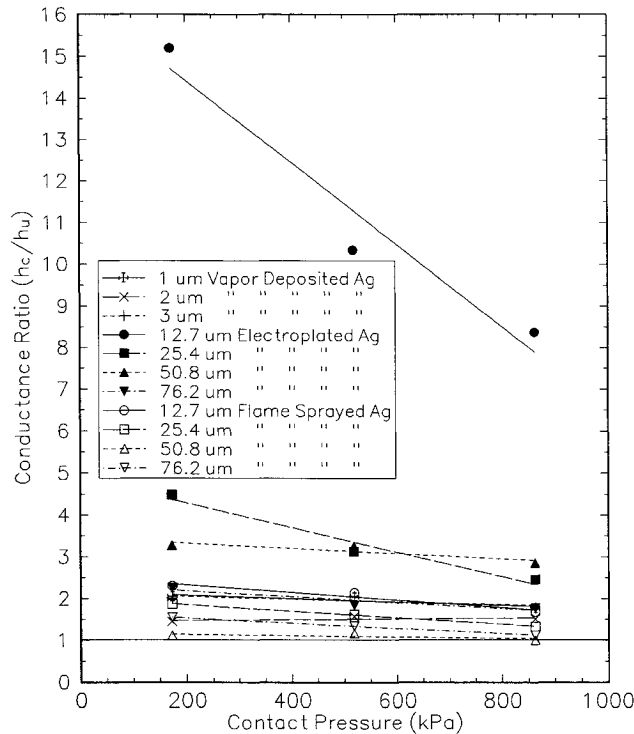


Fig. 7 Ratio of thermal contact conductance for anodized aluminum 6101-T6 to vapor-deposited, electroplated, and flame-sprayed silver-coated aluminum A356-T61 with respect to contact conductance for anodized aluminum 6101-T6 to bare aluminum A356-T61.

electroplated silver coatings afforded by far the greatest conductance enhancement, ranging from approximately 2.0 to 4.5 for the three thicker coatings (25.4, 50.8, and 76.2  $\mu\text{m}$ ), up to approximately an order of magnitude for the thinnest (12.7- $\mu\text{m}$ ) electroplated coating. The vapor-deposited silver coatings provided enhancement factors ranging from approx-

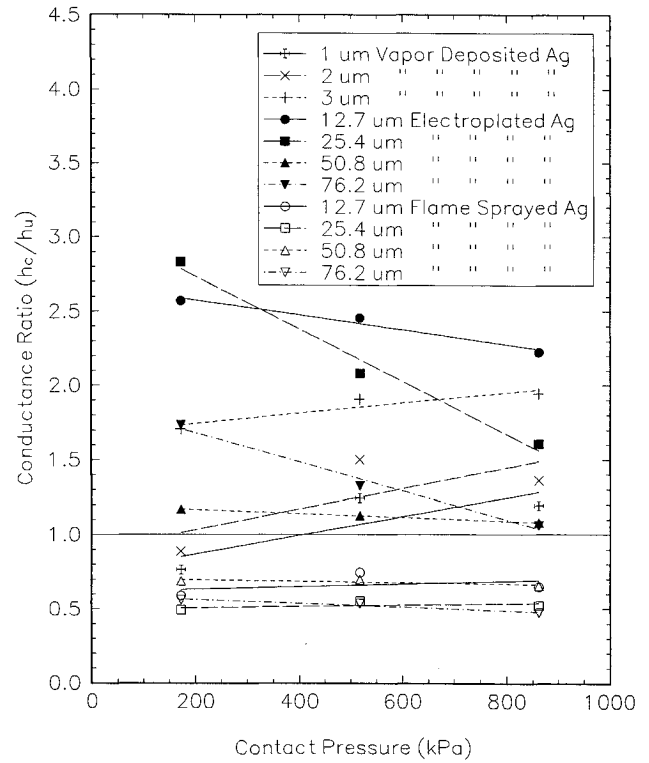


Fig. 8 Ratio of thermal contact conductance for electroless nickel-plated copper to vapor-deposited, electroplated, and flame-sprayed silver-coated aluminum A356-T61 with respect to contact conductance for electroless nickel-plated copper to bare aluminum A356-T61.

imately 1.5 to 2.1. The flame-sprayed silver coatings yielded enhancement ratios of about 1.1 to 2.3.

The contact conductance for electroless nickel-plated copper to vapor-deposited, electroplated, and flame-sprayed silver coated aluminum A356 with respect to the conductance for anodized aluminum 6101 to uncoated aluminum A356 is plotted in Fig. 8. Again, the electroplated silver coatings provided the greatest overall enhancement, varying from 1.1 to 2.8. The conductance ratios for the vapor-deposited silver coatings ranged from 0.75 to 2.2. The conductance ratios for the flame-sprayed silver coatings ranged from 0.45 to 0.75. That is, the flame-sprayed silver coatings caused reduced conductance.

#### F. Comparison with Theoretical Predictions

The experimental thermal contact conductance results for electroless nickel-plated copper to bare and silver-coated aluminum A356 were compared to Antonetti and Yovanovich's<sup>10</sup> theory for predicting the contact conductance of metallic coated metals, as illustrated in Fig. 9. Antonetti and Yovanovich's theory was developed for conforming (usually taken to mean optically flat), rough surfaces, whereas those surfaces employed in the present investigation often exhibited significant flatness deviations, since they were intended to be representative of typical commercially prepared surfaces. Flatness deviations lead to macroscopic gaps and significantly reduced conductance. Hence, the theory, since it deals only with microscopic contact resistance, should describe the upper bound to the data. Therefore, it is expected that the dimensionless conductance values for the present investigation should fall well below the prediction.

However, note from Fig. 9 that the dimensionless conductance values fall both above and below the theoretical prediction. This may be largely due to the value of thermal conductivity for the electroless nickel plating employed in calculations, 5.02 W/mK, as provided by Gawrilov.<sup>22</sup> This



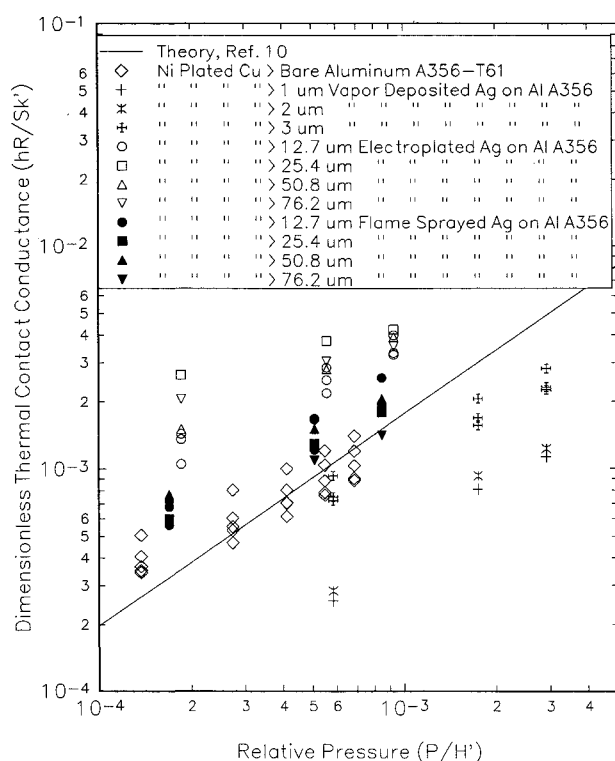


Fig. 9 Dimensionless thermal contact conductance vs relative pressure for electroless nickel-plated copper to bare and vapor-deposited, electroplated, and flame-sprayed silver-coated aluminum A356-T61.

value is more than an order of magnitude lower than the conductivity of commercially pure nickel (approximately 70 W/mK). Although the high phosphorus content of the electroless nickel plating (9.4% by weight) will certainly reduce the conductivity below the value for commercially pure nickel, the effect may not be as great as that reported by Gawrilov.<sup>22</sup> If the conductivity for commercially pure nickel is used, the dimensionless conductance is reduced by slightly more than an order of magnitude, thus displacing all data in Fig. 9 below the prediction as would be expected.

#### IV. Conclusions and Recommendations

This investigation was directed toward experimentally determining the thermal contact conductance of anodized aluminum 6101 and electroless nickel-plated copper frame materials to bare as well as vapor-deposited, electroplated and flame-sprayed silver-coated aluminum A356 card rail material. The conductance data for silver-coated aluminum A356 were compared to the baseline experimental results for uncoated aluminum A356 in order to determine the level of enhancement afforded by the silver coatings.

The electroplated silver coatings for the aluminum A356 card rail material provided substantial improvement of the conductance of junctions involving both the anodized aluminum 6101 and electroless nickel-plated copper. The vapor-deposited silver coatings usually made for increased conductance, whereas the flame-sprayed silver coatings enhanced the conductance of the junction with anodized aluminum 6101 and reduced the conductance of the junction with electroless nickel-plated copper.

In addition to possessing the best thermal enhancement characteristics, at least for this investigation, electroplated silver coatings are highly adherent, wear resistant, and impervious to corrosion in a marine atmosphere, as demonstrated by the salt spray test. Electroplated silver coatings are also relatively easily applied and fairly inexpensive. Aluminum A356 with thin coatings of vapor-deposited silver, as

used in this investigation, was found to be highly susceptible to galvanic corrosion in a marine atmosphere. However, thicker vapor-deposited silver coatings may prevent galvanic corrosion by completely masking the substrate. Flame-sprayed silver coatings, though quite durable, are highly porous, which may allow for galvanic corrosion if coatings are not thick enough to completely mask the surface.

The results for electroless nickel-plated copper to aluminum A356 were compared to the theory of Antonetti and Yovanovich<sup>10</sup> for conforming, rough metallic-coated metals. Some dimensionless conductance values for the present investigation were unexpectedly greater than predicted, although this may be due to an inordinately low estimate of the thermal conductivity of the electroless nickel plating.

It is recommended that electroplated and/or vapor-deposited silver coatings be evaluated for their suitability in supplanting the anodic coatings on aluminum 6101-T6 frames and the electroless nickel platings on copper frames.

#### Acknowledgments

Support for this study was provided by NSWC Contract N00164-91-C-0043 and the Center for Space Power at Texas A&M University, College Station, Texas.

#### References

- Kraus, A. D., and Bar-Cohen, A., *Thermal Analysis and Control of Electronic Equipment*, Hemisphere, New York, 1983.
- Williams, A., "Heat Transfer Across Metallic Joints," *Mechanical and Chemical Engineering Transactions*, Nov. 1968, pp. 247-254.
- Fletcher, L. S., "A Review of Thermal Enhancement Techniques for Electronic Systems," *IEEE Transactions on Components, Hybrids, and Manufacturing Technology*, Vol. 13, No. 4, 1990, pp. 1012-1021.
- Lambert, M. A., and Fletcher, L. S., "The Experimental Thermal Contact Conductance of Vapor-Deposited, Electroplated, and Flame Sprayed Silver Coatings," *Conduction Heat Transfer Lab., Dept. of Mechanical Engineering, Texas A&M University, Rept. CHTL-6770-13*, College Station, TX, Jan. 1993.
- Fried, E., "Study of Interface Thermal Contact Conductance," G. E. Valley Forge Space Technology Center, Summary Rept., G. E. Document 65S04395, Philadelphia, PA, 1965.
- Fried, E., and Kelly, M. J., "Thermal Conductance of Metallic Contacts in a Vacuum," *AIAA Paper 65-661*, Sept. 1965.
- Mal'kov, V. A., and Dobashin, P. A., "The Effect of Soft-Metal Coatings and Linings on Contact Thermal Resistance," *Inzhenerno-Fizicheskii Zhurnal*, Vol. 17, No. 5, 1969, pp. 871-879.
- Mikic, B. B., and Carnasciali, G., "The Effect of Thermal Conductivity of Plating Material on Thermal Contact Resistance," *American Society of Mechanical Engineers Transactions, Journal of Heat Transfer*, ASME Paper 69-WA/HT-9, Nov. 1969.
- O'Callaghan, P. W., Snaith, B., Probert, S. D., and Al-Astrabadi, F. R., "Prediction of Optimal Interfacial Filler Thickness for Minimum Thermal Contact Resistance," *AIAA Paper 81-1166*, June 1981.
- Antonetti, V. W., and Yovanovich, M. M., "Enhancement of Thermal Contact Conductance by Metallic Coatings: Theory and Experiment," *Journal of Heat Transfer*, Vol. 107, Aug. 1985, pp. 513-519.
- Antonetti, V. W., and Yovanovich, M. M., "Using Metallic Coatings to Enhance Thermal Contact Conductance of Electronic Packages," *Heat Transfer Engineering*, Vol. 9, No. 3, 1988, pp. 85-92.
- Kang, T. K., Peterson, G. P., and Fletcher, L. S., "Enhancing the Thermal Contact Conductance Through the Use of Thin Metallic Coatings," *American Society of Mechanical Engineers Transactions, Journal of Heat Transfer*, Vol. 112, No. 4, 1990, pp. 864-871.
- Chung, K. C., Sheffield, J. W., and Sauer, H. J., Jr., "Effects of Metallic Coated Surfaces on Thermal Contact Conductance: An Experimental Study," 6th Miami International Symposium of Heat and Mass Transfer, Miami Beach, FL, Dec. 1990.
- Chung, K. C., Sheffield, J. W., Sauer, H. J., Jr., and O'Keefe, T. J., "The Effects of Transitional Buffering Interface Coatings of Thermal Contact Conductance," *AIAA Paper 91-0490*, June 1991.
- Sheffield, J. W., Williams, A., Sauer, H. J., Jr., O'Keefe, T. J., and Chung, K. C., "Enhancement of Thermal Contact Conductance by Transitional Buffering Interfaces (TBI)," *National Science Foundation Final Project Rept., NSF Grant CTS-8901871* (Thermal



tems Program), Univ. of Missouri—Rolla, Rolla, MO, Jan. 1992.

<sup>16</sup>Lambert, M. A., and Fletcher, L. S., "Metallic Coatings for Enhancing the Thermal Contact Conductance of Electronic Modules," AIAA Paper 92-2849, July 1992.

<sup>17</sup>Ochterbeck, J. M., Peterson, G. P., and Fletcher, L. S., "Thermal Contact Conductance of Metallic Coated BiCaSrCuO Superconductor/Copper Interfaces at Cryogenic Temperatures," *American Society of Mechanical Engineers Transactions, Journal of Heat Transfer*, Vol. 114, No. 1, 1992, pp. 21–29.

<sup>18</sup>Lambert, M. A., and Fletcher, L. S., "A Review of the Thermal Contact Conductance of Junctions with Metallic Coatings and Films," AIAA Paper 92-0709, Jan. 1992.

<sup>19</sup>Lust, J. G., and Langford, A. B., "Update of Thermal Conductivity and Electrical Resistivity of Electrolytic Iron, Tungsten, and Stainless Steel," U.S. Dept. of Commerce/National Bureau of Standards, NBS Publication 260-90, Washington, DC, Sept. 1984.

<sup>20</sup>Touloukian, Y. S., and Ho, C. Y. (eds.), *Thermophysical Properties of Matter: Thermal Conductivity of Metallic Solids*, Vol. 1, Plenum Press, New York, 1972.

<sup>21</sup>Peterson, G. P., and Fletcher, L. S., "Measurement of the Thermal Contact Conductance and Thermal Conductivity of Anodized Aluminum Coatings," *American Society of Mechanical Engineers Transactions, Journal of Heat Transfer*, Vol. 112, No. 3, 1990, pp. 579–585.

<sup>22</sup>Gawrilov, G. G., *Chemical (Electroless) Nickel Plating*, Portcullis Press, Redhill, UK, 1979.

<sup>23</sup>Tabor, D., *The Hardness of Metals*, Oxford Univ. Press, Amen House, London, 1951.

<sup>24</sup>Darrow, G. R., "Engineering the Sulfuric Acid Process," *Anodized Aluminum*, American Society for Testing and Materials, ASTM STP 388, Philadelphia, PA, 1965, pp. 62–84.

<sup>25</sup>Krieg, A., "Processing Procedures," *Proceedings of the Symposium on Electroless Nickel Plating*, American Society for Testing and Materials, Philadelphia, PA, 1959, pp. 21–37 (ASTM STP 265).

<sup>26</sup>Macleane, J. D., and Korten, S. M., "A Practical Application of Electroless Nickel Plating," *Plating*, Vol. 41, No. 11, 1954, p. 1284.

<sup>27</sup>Sora, V., and Bollhalder, H., "Wear Reduction of Silver-Plated Sliding Contacts," *Plating and Surface Finishing*, Vol. 75, Jan. 1988, pp. 53–55.

<sup>28</sup>Blair, A., "Silver Plating," *Metal Finishing*, Vol. 88, No. 1A, Metals and Plastics Publications, Hackensack, NJ, 1990, pp. 268–272.

<sup>29</sup>"Standard Method of Salt Spray (Fog) Testing," American Society for Testing and Materials, ASTM B117, Vol. 7, Philadelphia, PA, 1973, pp. 60–67.

<sup>30</sup>Kline, S. J., and McClintock, F. A., "Describing Uncertainties in Single-Sample Experiments," *Mechanical Engineering*, Vol. 75, No. 1, 1953, pp. 3–8.

**Best Seller!**

# Fundamentals of Solid-Propellant Combustion

Kenneth K. Kuo and Martin Summerfield, editors

1984, 887 pp, illus, Hardback  
ISBN 0-915928-84-1  
AIAA Members \$74.95  
Nonmembers \$99.95  
Order #: V-90(945)

This book addresses the diverse technical disciplines of solid-propellant combustion. Contents include: Survey of Rocket Propellants and Their Combustion Characteristics; Perchlorate-Based Propellants; The Thermal Behavior of Cyclotrimethylenetrinitramine (RDX) and Cyclotetramethylenetetranitramine (HMX); Combustion of Metalized Propellants, and more.

Place your order today! Call 1-800/682-AIAA



American Institute of Aeronautics and Astronautics

Publications Customer Service, 9 Jay Gould Ct., P.O. Box 753, Waldorf, MD 20604  
FAX 301/843-0159 Phone 1-800/682-2422 9 a.m. - 5 p.m. Eastern

Sales Tax: CA residents, 8.25%; DC, 6%. For shipping and handling add \$4.75 for 1-4 books (call for rates for higher quantities). Orders under \$100.00 must be prepaid. Foreign orders must be prepaid and include a \$20.00 postal surcharge. Please allow 4 weeks for delivery. Prices are subject to change without notice. Returns will be accepted within 30 days. Non-U.S. residents are responsible for payment of any taxes required by their government.